Ocean Dynamics
DOI 10.1007/s10236-009-0181-x

Distributions and characteristics of dissolved organic matter in temperate coastal waters (Southern North Sea)

Andrea Lübben · Olaf Dellwig · Sandra Koch · Melanie Beck · Thomas H. Badewien · Sibylle Fischer · Rainer Reuter

Received: 28 August 2008 / Accepted: 29 January 2009

Abstract The spatial and temporal distributions of chromophoric dissolved organic matter (CDOM) and dissolved organic carbon (DOC) was studied in the East-Frisian Wadden Sea (Southern North Sea) during several cruises between 2002 and 2005. The spatial distribution of CDOM in the German Bight shows a strong gradient towards the coast. Tidal and seasonal variations of dissolved organic matter (DOM) identify freshwater discharge via flood-gates at the coastline and pore water efflux from tidal flat sediments as the most important CDOM sources within the backbarrier area of the Island of Spiekeroog. However, the amount and pattern of CDOM and DOC is strongly affected by various parameters, e.g. changes in the amount of terrestrial run-off, precipitation, evaporation, biological activity and photooxidation. A decoupling of CDOM and DOC, especially during periods of pronounced biological activity (algae blooms and microbial activity), is observed in spring and especially in summer. Mixing of the endmembers freshwater, pore water, and open sea water results in the formation of a coastal transition zone. Whilst an almost conservative behaviour during mixing is observed in winter, summer data point towards non-conservative mixing.

Keywords CDOM · Gelbstoff · DOM · DOC · Fluorescence · Wadden Sea · German Bight

Responsible Editor: Jörg-Olaf Wolff.

A. Lübben · T. H. Badewien · R. Reuter
Institute of Physics, Carl von Ossietzky University of Oldenburg,
26111 Oldenburg, Germany

O. Dellwig
Leibniz Institute for Baltic Sea Research,
18119 Rostock, Germany

S. Koch
Faculty of Technology,
University of Applied Sciences Fachhochschule Oldenburg/
Ostfriesland/Wilhelmshaven,
Constantiaplatz 4,
26723 Emden, Germany

O. Dellwig · M. Beck · S. Fischer
Institute for Chemistry and Biology of the Marine Environment,
Carl von Ossietzky University of Oldenburg,
26111 Oldenburg, Germany

A. Lübben (✉)
OceanWaveS GmbH,
Munstermannskamp 1,
21335 Lüneburg, Germany
e-mail: luebben@oceanwaves.de

1 Introduction

Chromophoric dissolved organic matter (CDOM), also denoted as gelbstoff or yellow substance, is the light-absorbing fraction of the dissolved organic matter (DOM) pool (Kalle 1938, 1949) and mainly results from the degradation of terrestrial and aquatic plant material. In the global biogeochemical carbon cycle, CDOM plays an important role due to its production and consumption by phytoplankton and bacteria. The absorption of CDOM affects the ocean colour and influences the underwater light field. Due to the absorption of CDOM, less radiation is available for photosynthesis which significantly affects aquatic ecosystems. Furthermore, the absorption of CDOM produces heat in the ocean (Kirk 1988). Regarding the entire pool of organic matter in the marine environment, CDOM amounts to a total of about 50–70% (Ertel et al. 1986; Spitzy and Ittekkot 1986). Depending on its origin and on the state of humification (Muller-Karger et al.

Published online: 17 March 2009

1989), CDOM is characterised by highly variable amounts of aromatic and unsaturated carbon groups (Hedges 1992; Malcolm 1990) whose molecular structure is not fully understood (Hedges et al. 2000). CDOM is commonly differentiated into humic and fulvic acids. For the freshwater environment of the study area, Gebhardt (2005) assigned 9–21% to the humic and 18–35% to the fulvic pool.

CDOM absorbs light in the ultraviolet (UV) and in the blue–green spectral region. The absorption coefficient, which is defined by a wavelength of 440 nm, decreases exponentially from the UV to the infrared (Bricaud et al. 1981; Green and Blough 1994; Kirk 1994). When excited at wavelengths in the UV, CDOM exhibits fluorescence with an emission maximum between 400 and 450 nm (Duursma 1974; Kalle 1949; Traganza 1969). The spectral position of this maximum increases with larger sizes of fluorescent molecules, and since terrestrial CDOM is composed of larger molecules, it fluoresces at higher wavelength than marine CDOM. Therefore, the optical spectroscopy of CDOM forms an important tool for identifying different water types (Determann et al. 1994; Nieke et al. 1997; Reuter et al. 1986) and enables estimates about sources and sinks of DOM (Coble et al. 1990; Mopper and Schultz 1993). In estuarine and most coastal regions, CDOM originating from terrestrial sources forms an essential part of the organic matter pool. By analysing terrestrial CDOM distributions, conservative or non-conservative mixing of different water masses can be identified (Coble 1996; de Souza Sierra et al. 1997; Reuter et al. 1993). For instance, Gueguen et al. (2005) reported both types of mixing for a similar run-off situation in the Western Arctic Ocean which seemingly depends on the sources of organic matter. Additionally, Hong et al. (2005) observed conservative mixing during the dry season in the Pearl River Estuary. As examples for the open ocean, fluorescence measurements by Vodacek et al. (1997) in the Middle Atlantic Bight and by Breves et al. (2003) in the Arabian Sea showed a linear mixing in deeper layers, and a non-linear mixing in surface waters due to photochemical degradation of CDOM. An overview about mixing processes and spectral characteristics of CDOM along with linear relationships of fluorescence and absorption is given by del Vecchio and Blough (2004) and references therein.

Regarding the CDOM budget, several factors as photodegradation, microbial production and decomposition of organic matter play an important role (Kouassi and Zika 1990; Miller and Moran 1997; Moran et al. 2000; Moran and Hodson 1994; Opsahl and Benner 1998). Additionally, lateral inputs as terrestrial run-off and pore water efflux have to be considered. The latter was investigated by Skoog et al. (1996), who observed the formation of CDOM fluorescence in the sediment and a flux across the sediment–water interface under anoxic conditions during laboratory experiments.

This study focuses on the CDOM distribution in the southern German Bight and the adjacent East-Frisian Wadden Sea with the major aim to provide a better understanding of the local coastal CDOM budget. For this purpose, tidal, seasonal and spatial variations of CDOM fluorescence, absorption coefficients and DOC in surface waters were investigated during several cruises between 2002 and 2005. Additionally, the DOM composition of the freshwater discharge via small coastal tributaries and the pore water system of the backbarrier tidal flats of the Island of Spiekeroog were analysed to locate sources and sinks and their influence on the mass balance of CDOM and DOC. Mixing processes of water types were identified by means of salinity whilst optical characteristics as fluorescence efficiency as well as fluorescence and absorption spectra allow conclusions about the origin of CDOM.

2 Material and methods

2.1 Study area

The North Sea forms a marginal sea of the North Atlantic Ocean characterised by a counter-clockwise cyclonic circulation due to the tidal regime, density gradients and major wind directions. The study area of this contribution forms the German Bight which is located in the SE part of the North Sea. Water types in the German Bight can be classified as follows: a tidal mixing zone with low salinities dominated by the terrestrial run-off, a transition zone with pronounced temperature and salinity gradients and the open North Sea water regime with higher salinity (Krause et al. 1986; Sündermann et al. 1999). The position of the transition zone varies depending on weather conditions and terrestrial run-off, with the latter dominated by four major rivers: Rhine, Elbe, Weser and Ems (Fig. 1a). Discharge volumes amount to about 2,524 m^3/s (Rhine), 80 m^3/s (Ems; WSV, http://www.wsv.de), 317 m^3/s (Weser; Global Runoff Data Centre, http://grdc.bafg.de) and 861 m^3/s (Elbe; ARGE Elbe, http://www.arge-elbe.de/).

In the southern German Bight, a chain of barrier islands, the East-Frisian Islands (Fig. 1a), is located which separates the open North Sea from the Wadden Sea ecosystem. The entire Wadden Sea spans from Den Helder in The Netherlands to Esbjerg in Denmark and comprises about 8,000 m^2 thereby forming the largest connected intertidal ecosystem of the world. The average distance between the mainland and the islands is about 8 km and tidal inlets between the islands have a width of about 1 to 3 km. The Wadden Sea environment with its semidiurnal tides forms a highly dynamic ecosystem due to physical forcing (e.g. changing water level) and seasonal variability of biological activity.

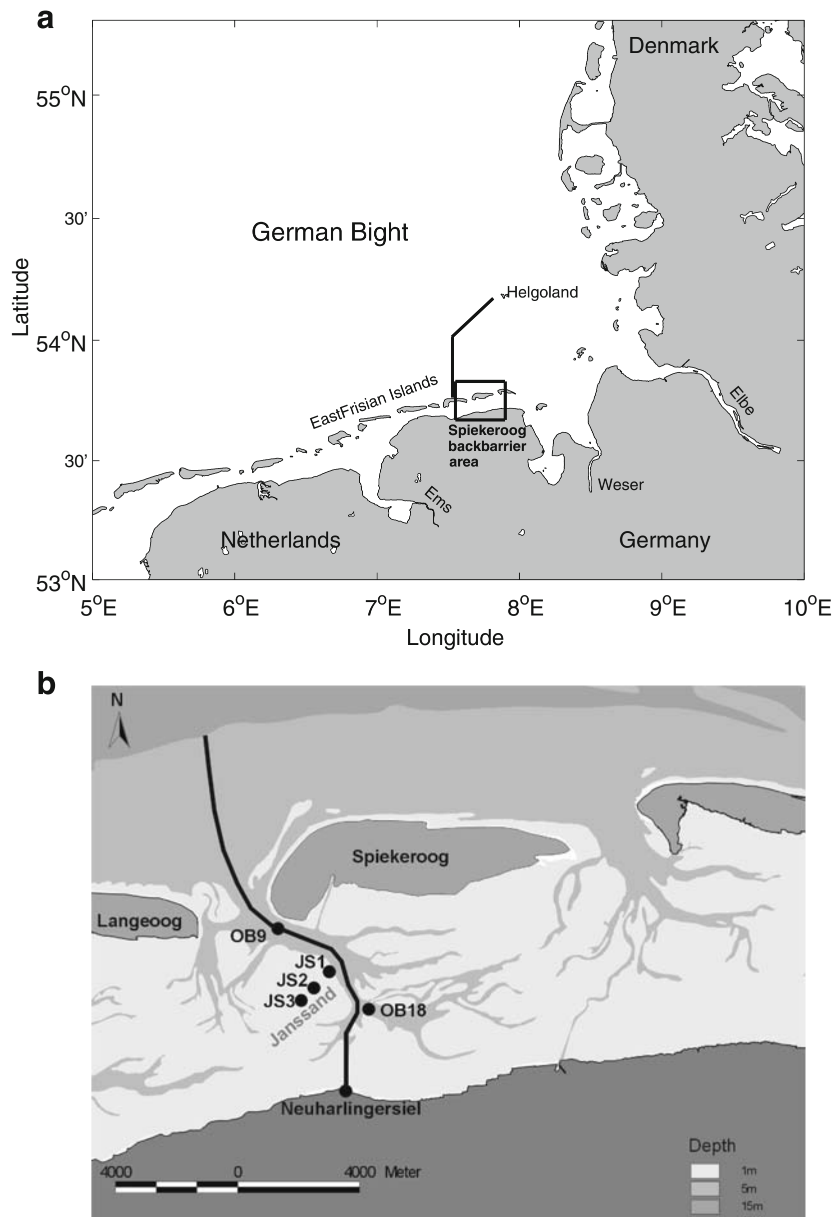

Fig. 1 a Map of the major study area in the southern German Bight. The *black line* indicates a transect towards the Island of Helgoland during a cruise with R/V Heincke in July 2005. **b** Detailed map of the Spiekeroog backbarrier tidal flat with locations of time series at sites OB9 and OB18. The *black line* denotes transects across the main tidal channel. JS1, JS2 and JS3 indicate the location of pore water sampling sites

The major study area of this contribution forms the backbarrier area of Island of Spiekeroog (Fig. 1b). Here, the high water volume amounts to about 145×10^6 m^3, whereas at low tide a water volume of about 40×10^6 m^3 remains. These results in a tidal water exchange volume of approximately 105×10^6 m^3. During ebb tide, the tidal flats fall dry and only the deeper channels are still filled with water. The pore waters, which drain out of the sediments during ebb tide, contribute significant amounts of trace metals, nutrients and organic components to the open water column (Beck et al. 2008a, b; Billerbeck et al. 2006a, b; Dellwig et al. 2007a, b). The outflow of the Wadden Sea waters through the tidal inlets occurs in the northwest direction following the bottom topography and joining the general eastward circulation further north. The water level is changing within the tidal cycle by about 2–3 m with current velocities of up to approximately 2 m/s. Thus, the residence time of water in the backbarrier area is about three tidal cycles as reported by Shaw (2003) and Stanev et al. (2003), who investigated the flushing time on the basis of Ra isotopes and numerical modeling, respectively. Comparable results are derived from a Lagrangian model calculation (Wolff and Flemming 2003), which estimates the residence time of water to be about two tidal cycles in the region of the tidal inlets and deeper channels and about 20 tidal cycles for the water north of the islands close to the coast.

Terrestrial run-off enters the backbarrier tidal flats of the Island of Spiekeroog via flood-gates located in Neuharlingersiel, generally about 2 h before low tide when the water level of the hinterland is above sea level (Fig. 1b). The drainage volume (averaging 15×10^6 m^3 in winter and 9×10^6 m^3 in summer; NLWKN 2000, 2004) depends on precipitation in the catchment area, which covers about 125 km^2 for the floodgates in Neuharlingersiel.

The tidal flat sediments of the backbarrier area of Island of Spiekeroog consist of sand, mud and mixed flats with sand flats forming the dominating facies. Whilst mud flats are characterised by higher clay content and, therefore, by a lower porosity (Flemming and Zeigler 1995), the permeable sand flat sediments favour the exchange of pore water with the open water column and enhance water transport within the sediment, respectively.

2.2 Sample collection

Figure 1a and b shows the sampling sites in the study area which consist of a transect off the Island of Langeoog towards the Island of Helgoland, a transect from the harbour of Neuharlingersiel towards the open sea and the two time series stations OB9 and OB18 in the backbarrier tidal area of the Island of Spiekeroog. Surface waters were taken with a stainless steel metal bucket. Samples used for absorption and fluorescence spectroscopy were immediately filtered through pre-combusted (450°C for 6 h) glass fibre filters (Schleicher & Schüll GF50, 0.45 µm pore size; since July 2005 Whatman/Schleicher & Schüll GF/F, 0.7 µm pore size) and stored in clean amber-coloured glass bottles. The filtered samples were analysed immediately on board ship, at the latest within 1 h after sampling.

Samples of the terrestrial run-off were filtered as well through pre-combusted (450°C for 6 h) glass fibre filters (Schleicher & Schüll GF50, 0.45 µm pore size) and stored cool and dark until measurement in the laboratory.

Additionally, pore water sampling was carried out at three sites on the Janssand sand flat on a transect from the central part of the tidal flat (JS3) towards the low water line close to the main tidal channel (JS1). Sampling was performed by using permanently installed pore water lances (Beck et al. 2007) which reach a sediment depth of about 5 m and enable sampling from 20 different depths. The distance between sites JS1 and JS2 is 800 m and between JS2 and JS3 is 500 m. The pore water samplers consist of a PVC liner with several sampling ports in specific depths. These ports are covered with gauze to prevent the penetration of sediment material. The ports are connected via Teflon tubes to the sediment surface. Pore water sampling can be done by connecting syringes on the top of the sampler. CDOM samples were immediately filtered through pre-combusted (450°C for 6 h) glass fibre filters (GF/F, 0.7 µm pore size) into amber-coloured glass bottles. Samples were stored cool and dark until measurements in the laboratory within 12 h after sampling.

2.3 Fluorescence spectroscopy

Samples were measured with a Shimadzu RF1500 fluorescence spectrophotometer. With an excitation wavelength of 308 nm, the emission was scanned from 320 to 550 nm in 1 nm intervals. The instrument was used with a spectral resolution of 10 nm. Flow-through quartz cuvettes with 1 cm path length were used. They were cleaned first with Mucasol® soap, then stored in 20% HNO_3 and soaked again in Mucasol®. Between and after these procedures, the cuvettes were rinsed with purified water.

The spectra were corrected for electronic offset signals with reference spectra from purified water at the same excitation wavelength to avoid instrumental instabilities. The excitation side of the spectrometer was calibrated with an excitation scan of dye (Rhodamine B). A spectral calibration in the UV range of the emission side of the instrument was done with a synchronous scan. For the visible region, quinine sulphate dihydrate in 0.1 mol/L $HClO_4$ was measured and the relation to a reference spectrum provided by the American National Institute of Standards and Technology (Velapoldi and Mielenz 1980) was calculated.

Normalisation was done by determining the area of the water Raman scattering band from the purified water scans and dividing every data point in the sample spectra by this area. Due to the constant Raman scattering of purified water, this leads to instrument-independent fluorescence intensity, the Raman unit (Determann et al. 1994). Reference measurements with purified water were performed every eight samples. For the measurements described in this study, the relative accuracy is estimated to be <5%. Due to a lack of spectral correction procedures in the years 2004 to 2005, an error of up to about 10% at the defined wavelength of 420 nm is expected for these years. In the investigated backbarrier area of Spiekeroog, CDOM shows the most intensive fluorescence at an emission of about 420 nm, when excited at a wavelength of 308 nm. These excitation/emission wavelengths are used to quantify CDOM fluorescence in this paper.

2.4 Absorption spectroscopy

Absorbance was measured with a double-beam Perkin Elmer Lambda 18 photometer over a range from 200 to 800 nm. Samples taken in the German Bight were measured on board within the next hour using customised 10 cm stainless steel cuvettes with quartz windows. Samples from the Wadden Sea were frozen immediately after filtration and measurements were done in the home laboratory using a 1-cm quartz cuvette.

The measured absorbance readings $A(\lambda) = \log\left(I_{\mathrm{reference}}/I_{\mathrm{sample}}\right)$ were converted to absorption coefficients $a(\lambda) = \ln\left(I_{\mathrm{reference}}/I_{\mathrm{sample}}\right)/r$ according to:

$$a(\lambda) = 2.303 \times A(\lambda)/r \tag{1}$$

in 1 nm intervals where $I_{reference}$ and I_{sample} are the reference and sample signal intensities and r is the path length of the cuvette.

The cuvettes were cleaned the same way as for fluorescence spectroscopy. The reference cuvette was filled with purified water for compensation of absorption and instrumental sensitivity. Baseline correction was done approximately every tenth data acquisition. Due to the sample filtration with pre-combusted Millipore® GF/F glass fibre filters having a nominal pore width of 0.7 μm, the measured data are assumed to represent absorption of the CDOM fraction. The instrumental resolution is 0.002 m^{-1}, the relative accuracy of the data after exclusion of outliers is estimated at 10% with $a<0.1$ m^{-1} and 3% above.

Due to the chosen fluorescence excitation wavelength, the absorption coefficient at 308 nm was also taken for an index of CDOM quantity. This allows a direct comparison of these parameters and especially a calculation of fluorescence efficiencies of the CDOM.

To avoid errors during filtration of samples for absorption measurements and instrumental long-term drift of the photometer, which lead to scattering and baseline fluctuation, the absorption coefficient at 700 nm was subtracted from the coefficient measured at 308 nm (Bricaud et al. 1981). Samples with values higher than 0.5 m^{-1} at 700 nm were considered as outliers and excluded from the dataset.

Because of the high amounts of DOM found in the Wadden Sea, the samples were tested with the absorption photometer in order to investigate the risk of self-absorption of fluorescence in the sample cuvette during fluorescence measurements. With the help of dilution series, an absorption coefficient of approximately $a=40$ m^{-1} at 308 nm using 1 cm cuvettes was made out to be the lower limit for significant self-absorption of CDOM for samples from the investigated area.

2.5 Dissolved organic carbon

Sub-samples of 50 mL were filtered through pre-combusted GF/F (Whatman) filters aboard. Samples were acidified to pH 2 by HCl. The filtrate was stored at 4°C in brown glass bottles until analysis within 1 week. DOC concentrations were determined after high-temperature oxidation by a multi N/C 3000 analyser (Analytik Jena, Germany). Potassium hydrogen phthalate was used as external standard. Accuracy (0.4%) and precision (4.6%) of the DOC measurements were tested by replicate analysis of freshly prepared K-hydrogen phthalate solutions.

2.6 In situ CTD measurements

Temperature and salinity were measured with a CTD mounted on a rosette water sampler. Two different research vessels were used depending on the water depth of the sampling site. In the region of the backbarrier area, a SeaBird Electronics model SBE19plus was used on board R/V Senckenberg. The accuracy is <0.005°C for temperature and <0.001 for salinity calculated from conductivity, temperature and pressure. The absolute accuracy and resolution of the pressure sensors is <0.1 dbar. In the sampling area of the German Bight aboard R/V Heincke, a ME Meerestechnik-Elektronik GmbH model OTS 3000 was employed. Temperature and pressure were measured with an accuracy of <0.01°C and 0.2 dbar, respectively. Salinity data were determined at an accuracy of <0.02.

3 Results and discussion

3.1 Tidal and spatial variation of DOM in the Wadden Sea

The tidal variation of CDOM fluorescence and DOC is presented in Fig. 2 for the two time series locations (OB9 and OB18) in January 2004 (see Fig. 1b). At station OB 9, which is located near the tidal inlet, a tidal cyclicity is obvious with maximum values during low tide indicating the tidal flat environment as an important source (Fig. 2, left). CDOM fluorescence intensities are ranging from 0.09 Raman units/nm during high tide to 0.15 Raman units/nm during low tide at position OB9. In the central backbarrier area at station OB18 (Fig. 2, right), this tidal pattern is observed as well, with somewhat higher CDOM fluorescence values (0.10 to 0.19 Raman units/nm). However, at this site, the pattern is superimposed by the discharge of organic-rich freshwater via the flood-gates in Neuharlingersiel as reflected in strongly decreasing salinity shortly after low tide. Here, the freshwater is already mixed with sea water, having a salinity of about 15, which is approximately half the open sea water salinity. Correspondingly, CDOM fluorescence and DOC increase by approximately a factor of 2 in the diluted freshwater.

A comparable behaviour of CDOM fluorescence, DOC, salinity and temperature is seen about 2 h after high tide at station OB9 as well (Fig. 2, left), but much less pronounced. Drifter experiments in this area showed that discharge plumes reach the tidal inlet not directly within one tidal cycle (Dellwig et al. 2007a; Puncken et al. 2006). After discharge through the flood-gate, the freshwater plume arrives in the central backbarrier area at low tide. In the following flood tide, it is transported backwards in direction to the coast. Afterwards in the consequent ebb tide, this water mass reaches the tidal inlet highly diluted.

Figure 3 presents the same parameters at the same positions over one tidal cycle from 19 to 20 July 2005, but without terrestrial run-off via the flood-gates since 14 July 2005. Thus, the last freshwater input is about more than

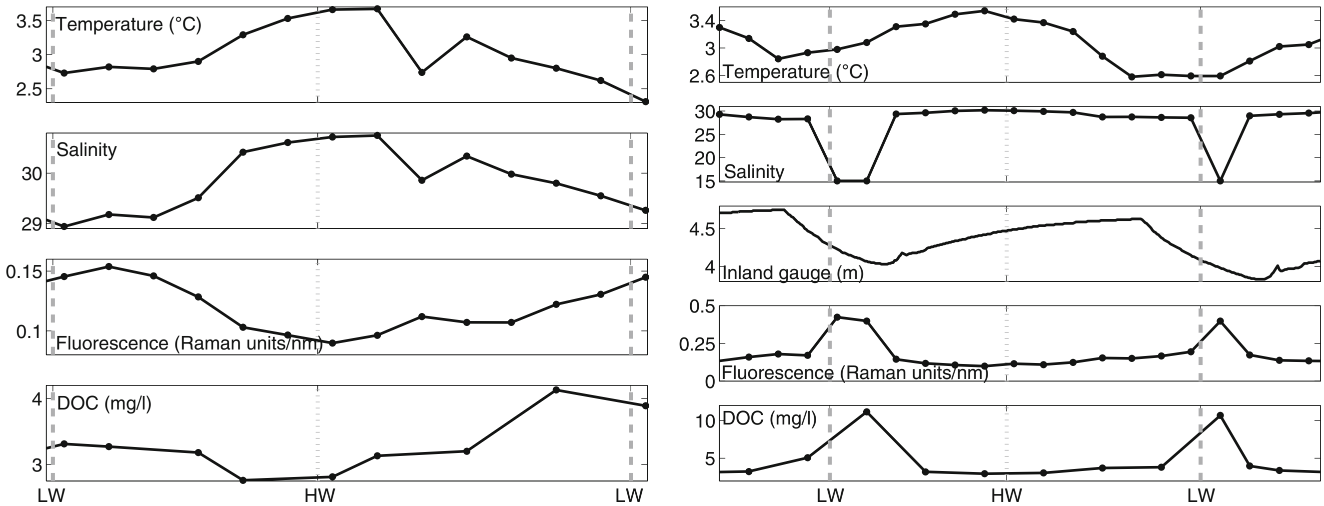

Fig. 2 Tidal cycle of temperature, salinity, fluorescence (λ_{ex}=308 nm, λ_{em}=420 nm) and DOC in the backbarrier area at position OB9 (see Fig. 1b) on 21 January 2004 (*left*) and at position OB18 (see Fig. 1b) on 20 January 2004 (*right*)

seven tidal cycles ago. Due to the known residence time of water in the backbarrier area of three tidal cycles, a direct influence of the terrestrial run-off on DOM can be excluded during this time period. Nevertheless, a tidal cyclicity of CDOM fluorescence and DOC is seen; even though less pronounced. This behaviour points towards an additional source of organic matter which cannot be attributed to the terrestrial run-off only. Such assumption is in accordance with the irregular pattern and small range (0.2) of salinity which reflects the lack of freshwater input.

Figure 4 shows the spatial distribution of CDOM fluorescence and DOC along with salinity and temperature for two transects from Neuharlingersiel towards the Island of Spiekeroog (see Fig. 1b). These transects were carried out during high tide and low tide on 7 February 2005. Terrestrial run-off occurred twice a day in the week before. The decrease in salinity to <1 during low tide indicates a significant freshwater contribution due to the opening of the flood-gates. This freshwater is highly enriched in organic compounds as seen in elevated values of CDOM fluorescence. In contrast, only a slight increase is observed close to the harbour during high tide. The CDOM fluorescence in the harbour is about four times higher at low tide compared to high tide. Almost similar values during high and low tide of the remaining samples are most likely caused by intense mixing of Wadden Sea waters as the freshwater is subsequently diluted with sea water.

Comparable results of the distribution of CDOM in coastal regions were found e.g. in the Northern Gulf of Mexico by Conmy et al. (2004). The authors reported a

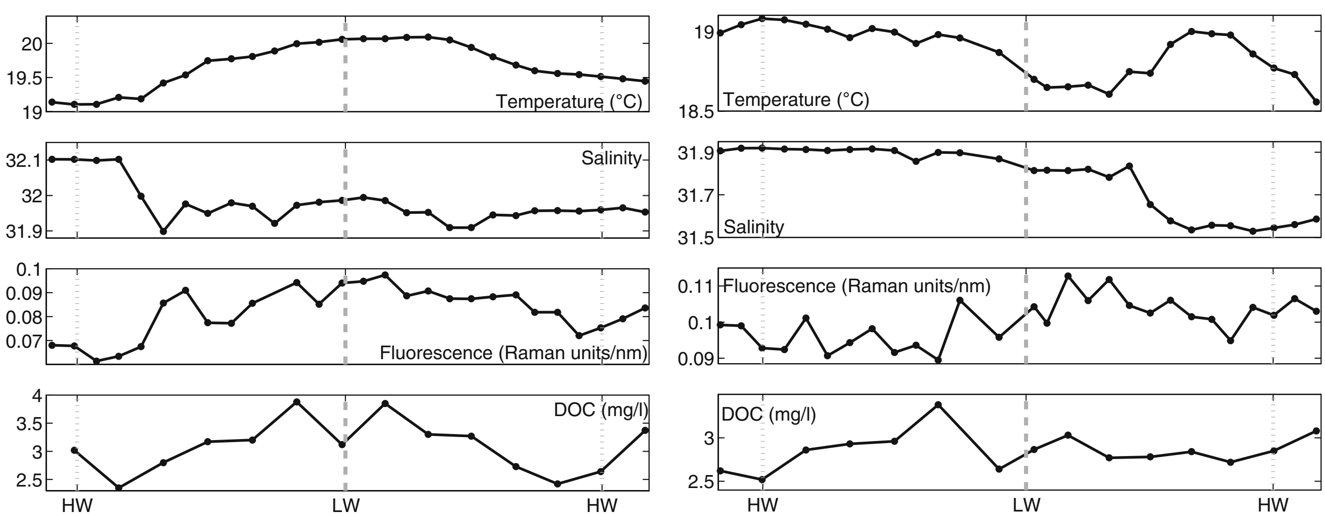

Fig. 3 Tidal cycle of temperature, salinity, inland water level, fluorescence (λ_{ex}=308 nm, λ_{em}=420 nm) and DOC in the backbarrier area at position OB9 (see Fig. 1b) on 19 July 2005 (*left*) and at position OB18 (see Fig. 1b) on 20 July 2005 (*right*)

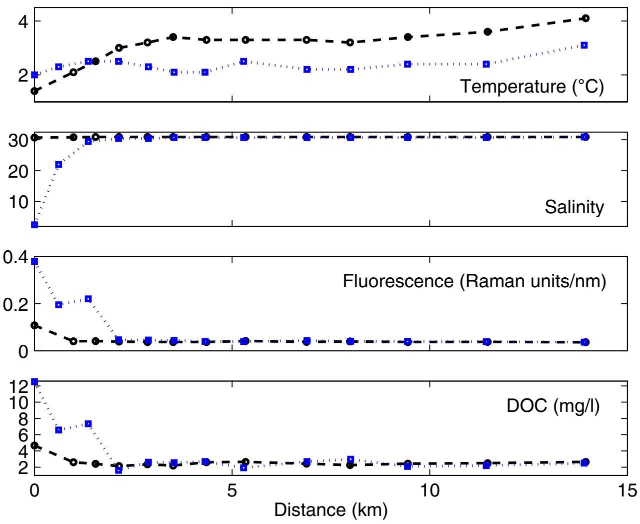

Fig. 4 CDOM fluorescence (λ_{ex}=308 nm, λ_{em}=420 nm), DOC, temperature and salinity measured along the Wadden Sea transect during high water (*black dashed line and circles*) and low water (*blue dotted line and squares*) on 7 February 2005. The transect starts in the harbour of Neuharlingersiel and ends about 10 km off the tidal inlet

similar influence of terrestrial run-off on the coastal CDOM fluorescence. Although the freshwater run-off was highly variable in their study area, the riverine input was always the primary factor controlling CDOM fluorescence. This dominating influence of river run-off was also evidenced by Chen and Gardner (2004) who pointed out the importance of the rivers Mississippi and Atchafalaya for the northern Gulf of Mexico. Further investigations with similar results were done in the St. Lawrence Estuary (Nieke et al. 1997), in the Middle Atlantic Bight (Del Vecchio and Blough 2004), in the Tampa Bay (Chen et al. 2007) and in the Pearl River Estuary (Callahan et al. 2004).

3.2 Seasonal variation of DOM in the Wadden Sea

The variability of CDOM fluorescence, DOC and salinity obtained in a series of cruises over 4 years is presented in Fig. 5a–c. Each dataset represents the mean value and standard deviation of one complete tidal cycle in the backbarrier area at position OB9 (see Fig. 1b). These data are completed by monthly means of terrestrial run-off via the flood-gates at Neuharlingersiel (Fig. 5d). Unfortunately, there is a data gap for run-off volumes in 2004, which has been substituted by data from the westerly flood-gate about 15 km afar.

CDOM fluorescence shows a seasonal dependence with higher and more scattered values in winter whereas the summer values are generally lower and encompass a smaller range most likely due to the lower fluorescence of marine DOM and reduced terrestrial input. Salinity exhibits an inverse pattern compared to CDOM fluorescence with generally higher values during spring and summer when freshwater contribution is low and evaporation is high. An extreme example was observed in August 2003 when salinity was higher during low tide when compared with the high tide level. Furthermore, high radiation in summer

Fig. 5 a–d Mean values and standard deviation of CDOM fluorescence (λ_{ex}=308 nm, λ_{em}=420 nm), DOC, salinity (all measured over one tidal cycle at position OB9 in the backbarrier area, see Fig. 1), and the monthly run-off volume at the flood-gates in Neuharlingersiel

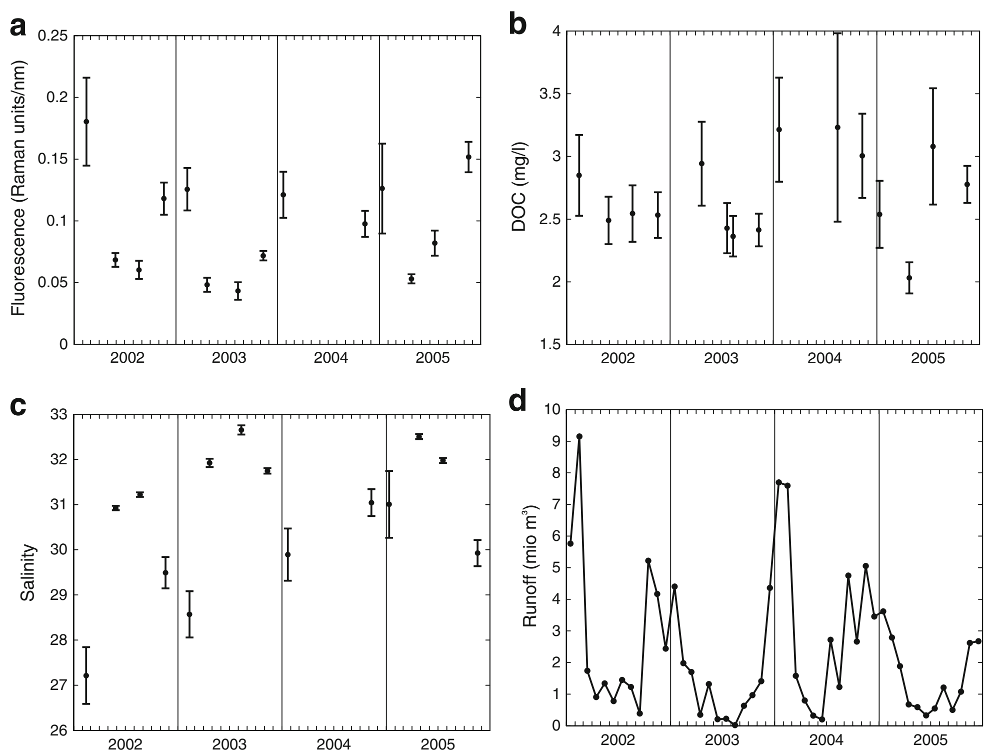

enhances chemical photodegradation thereby also reducing the fluorescence level (Determann 1995). In contrast, elevated terrestrial run-off contributes higher amounts of CDOM as evidenced by a positive correlation between both parameters (r=0.78). Such a clear seasonal pattern is not observed for DOC. In addition to freshwater contribution, DOC is also highly influenced by biological activity. Thus, DOC is released during growth and lyses of algae (Dellwig et al. 2007b) and subsequently degraded and/or modified by bacteria. Although DOC shows high values in winter, the spring and summer data are highly variable and reflect no seasonal dependency. For instance, summer data from July 2005 comprise a larger range when compared with August 2003. This reflects the influence of phytoplankton blooms and the release of organic compounds. Samples in July 2005 were taken during the breakdown of an algae bloom, whilst in August 2003 phytoplankton activity was relatively low (Dellwig et al. 2007b). These authors showed that elevated ratios of phaeopigments and chl-a in July 2005 are in accordance with the breakdown of an algae bloom and degradation of freshly formed organic matter. Pronounced microbial activity in the water column has been identified by elevated cell numbers of free-living and aggregate-associated bacteria. The relevance of microbial activity in summer was already observed for other parameters as redox-sensitive trace metals, aggregate size and abundance, particulate organic matter, chl-a and bacterial production (Dellwig et al. 2007b; Lunau et al. 2006). Especially, aggregation favours the transfer of DOM into the particulate phase as well as deposition and burial in the sediments. Thus, large organic-rich aggregates are formed during phases of algae blooms and elevated bacterial activity (Dellwig et al. 2007b; Lunau et al. 2006), respectively. As such, aggregates behave hydraulically different than smaller inorganic particles; they are deposited on the tidal flat sediments (Chang et al. 2006). Once deposited, aggregates are buried in the first centimetres of the sediments due to advective water flow in surface sediments (Huettel and Rusch 2000; Huettel et al. 1998) and bioturbation (Volkenborn et al. 2007). Subsequently, aggregates are microbially remineralised and particulate organic matter is again transferred into the dissolved phase. This transfer of organic material seems to be especially important in April 2005 when extremely low levels of DOC were found in the Wadden Sea. Furthermore, generally low CDOM values between March and August may also be strengthened by the aforementioned process of aggregation.

Overall, the seasonal comparison of CDOM fluorescence and DOC reflects a decoupling of both parameters during periods of elevated (micro)biological activity and documents the different seasonal behaviours of these parameters. Therefore, different cycles, sources, sinks and budgets have to be taken into account. A finding that was also indicated by Del Vecchio and Blough (2004), who investigated the distribution and behaviour of CDOM and DOC in the Middle Atlantic Bight. Due to varying CDOM/DOC ratios, these authors assumed a decoupled behaviour of both parameters.

3.3 Sources and sinks of DOM in the Wadden Sea

3.3.1 German Bight

In July 2005, a transect was carried out from the Island of Langeoog to the Island of Helgoland (Fig. 6, see Fig. 1a), in order to follow the outflow of the coastal waters into the German Bight. Sampling started at the Island of Langeoog at about 3 h after low tide and lasted about 6 h. A clearly decreasing gradient of fluorescence and absorption is evident from land to sea with 0.07 Raman units/nm near the coast and 0.03 Raman units/nm further offshore (54°03′ N; 007°37′ E). Thus, signals of Wadden Sea waters are observed until a distance of about 20 km of the islands. At this position, water temperature and salinity reach their minimum/maximum levels, thereby indicating leaving of direct coastal influences. Close to the Island of Helgoland, the fluorescence slightly increases again reaching a value of 0.04 Raman units/nm, which is probably caused by run-off of the River Elbe. A similar pattern is observed for 308 nm absorption coefficients which vary from a maximum of 3.2 m^{-1} close to the coast to an offshore minimum value of 1.5 m^{-1}. Both optical parameters are in accordance with DOC which shows highest values close to the Island of Langeoog and increasing values further offshore.

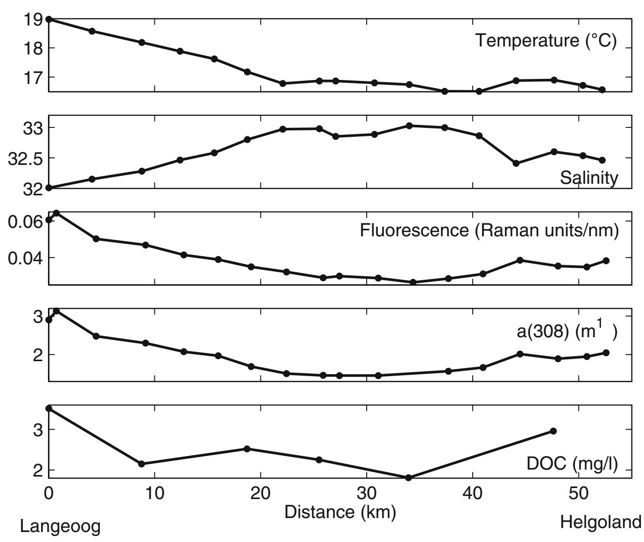

Fig. 6 Distribution of salinity, temperature, CDOM fluorescence (λ_{ex}= 308 nm, λ_{em}=420 nm), absorption coefficient (308 nm) and DOC along a transect in the German Bight on 20 July 2005. The transect starts near the island of Langeoog and ends at the island of Helgoland

3.3.2 Terrestrial run-off

Along with decreasing salinity, the gradient of increasing CDOM fluorescence and DOC values from the German Bight towards the coastline (see Figs. 4 and 6) implies the importance of a terrestrial DOM source. On the mainland side of the flood-gates and in the freshwater tributaries flowing towards Neuharlingersiel, DOC endmember values range from 12.2 to 22.8 mg/L with a mean concentration of 15.0 mg/L for 54 samples taken between 2002 and 2003. This freshwater DOC varies throughout the year, but does not follow a seasonal pattern. The mean freshwater DOC content is about six times higher than the mean concentration observed in the backbarrier area. The CDOM fluorescence of the freshwater endmember is on average 1.02 Raman units/nm ranging between 0.73 and 1.26 Raman units/nm (Kölsch et al. 2003).

Depending on the mean terrestrial run-off volumes (see Fig. 5), monthly and yearly mean DOC mass transports can be estimated roughly. Consequently, the monthly mean DOC input due to terrestrial discharge via the flood-gates varies between 0.3×10^6 g in August 2003 and 137×10^6 g in February 2002. The resulting annual DOC input constitutes 519×10^6, 264×10^6, 570×10^6 and 277×10^6 g for the years 2002 to 2005 when considering the respective annual run-off volumes of 34.6×10^6, 17.6×10^6, 38.1×10^6 and 18.5×10^6 m^3. The mean water volume entering and leaving the backbarrier area during each tidal cycle is about 105×10^6 m^3. Considering the amount of DOC, which is higher in the outflowing water (about 3 mg/L) in contrast to the concentration found in the incoming water of approximately 2 mg/L, the annual total mean output of DOC is estimated to be about 74×10^9 g. This value is three orders of magnitude higher in comparison to the DOC input via the freshwater, thus again pointing towards another important organic matter source in the Wadden Sea. This source is assumed to be the pore water of the tidal flat sediments which will be discussed in the following section.

3.3.3 Pore water

Figure 7 presents CDOM fluorescence and DOC in pore waters of sandy sediments from the Janssand site (JS; see Fig. 1b) taken on 24 and 25 April 2006 during low tide. Generally, CDOM fluorescence and DOC increase with depth. At all three sites, CDOM fluorescence in the uppermost sample shows values from 0.21 to 0.24 Raman units/nm which is two times higher than the corresponding mean values of the overlying water column (0.09–0.12 Raman units/nm). Below, CDOM fluorescence decreases on average to 0.15 Raman units/nm at about 0.2 m depth. Further down, CDOM fluorescence increases continuously, with about 25 times higher values at 5.0 m depth when compared with the open water column. DOC concentrations show a similar pattern with depth and along the transect. In surface sediments, DOC concentrations are similar or slightly higher than those of the open water column. Below the surface, DOC increases with depth. However, at site JS1, the pronounced increase is much stronger; reaching a maximum of about 26.0 mg/L. Additionally, an unexpected minimum is found at 4.0 m depth at site JS2.

CDOM fluorescence and DOC both show a gradient towards the tidal channel, with increasing concentrations in margin sediments. This suggests that CDOM-rich and DOC-rich pore waters may represent a source when released to the open water column. Pore water flow induced during low tide in tidal flat margin sediments lead to pore water seeps in these sediments. Draining pore waters contribute significantly to the nutrient and trace metal reservoir of the open water column (Billerbeck et al. 2006b;

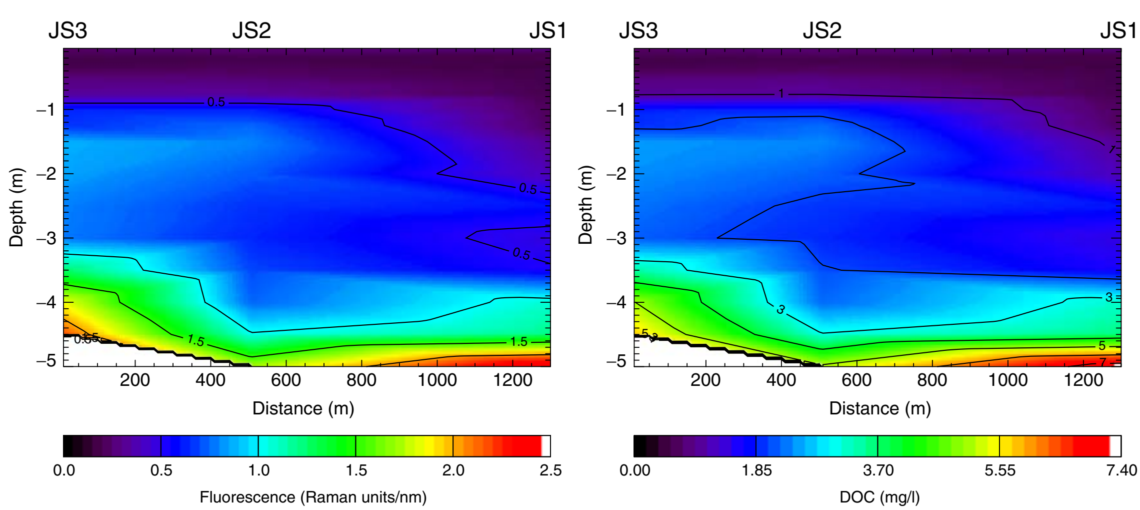

Fig. 7 CDOM fluorescence (λ_{ex}=308 nm, λ_{em}=420 nm, *left*) and DOC (*right*) pore water profiles in April 2006 at JS sites

Niesel and Günther 1999; Dellwig et al. 2007a, b). Beck et al. (2008c) estimated the outflow of surface and deep pore waters into the open water column based on manganese datasets. The authors calculated a contribution of deep pore waters to the overall manganese budget of the backbarrier tidal flat of less than 4%, whereas the surface flow amounts to about 80%. The latter is in accordance with the results of Dellwig et al. (2007a), who determined the influence of seeping pore waters to the manganese budget of about 90%.

The importance of pore water seepage is reported for various parameters and environments. Skoog et al. (1996) investigated CDOM fluorescence in pore water of coastal marine sediments of the Gullmar Fjord in western Sweden with in situ benthic chambers and laboratory tank incubations. CDOM fluorescence was formed in the sediment and a flux across the sediment–water interface occurred under anoxic conditions. This pore water flux out of surface sediments was also observed in the East-Frisian Wadden Sea (Billerbeck et al. 2006b).

Monthly pore water sampling between summer 2005 and summer 2006 at site JS1 shows varying CDOM fluorescence values. These variations occur especially at a depth of 2.5 m, where permeable sandy sediments are situated (Beck et al. 2008a). At this depth, sampling over a tidal cycle further revealed that CDOM fluorescence is not constant and varies between 0.04 and 0.83 Raman units/nm. In order to clarify these pore water dynamics in detail, further analysis of these data is in progress.

Overall, discharge of DOM-rich pore waters from surface and deep sediment layers to the open water column presumably represents an important source for the entire Wadden Sea DOM budget. This finding is in accordance with tidal patterns of DOM, i.e. increasing values observed during low tide in the backbarrier area. Pore water efflux explains the tidal pattern seen in Fig. 3 during periods without terrestrial run-off. Thus, DOM is released continuously during every low tide by deep pore water advection. The efflux from surface sediments by pore water advection depends on the season. Discharge via freshwater accounts for a rather pulse-like supply in DOM.

3.4 Mixing processes and water types

In order to investigate mixing processes of different water masses in the study area, Fig. 8 shows the relationship between CDOM fluorescence, absorption coefficients and salinity. Figure 8a and c shows the CDOM fluorescence versus salinity for the German Bight and the backbarrier area of Spiekeroog in winter (16 to 20 March 2005) and summer (18 to 20 July 2005), whereas in Figure 8b and d, the absorption coefficients are presented for the German Bight in winter (11 to 13 January 2005) and summer (18 to 20 July 2005).

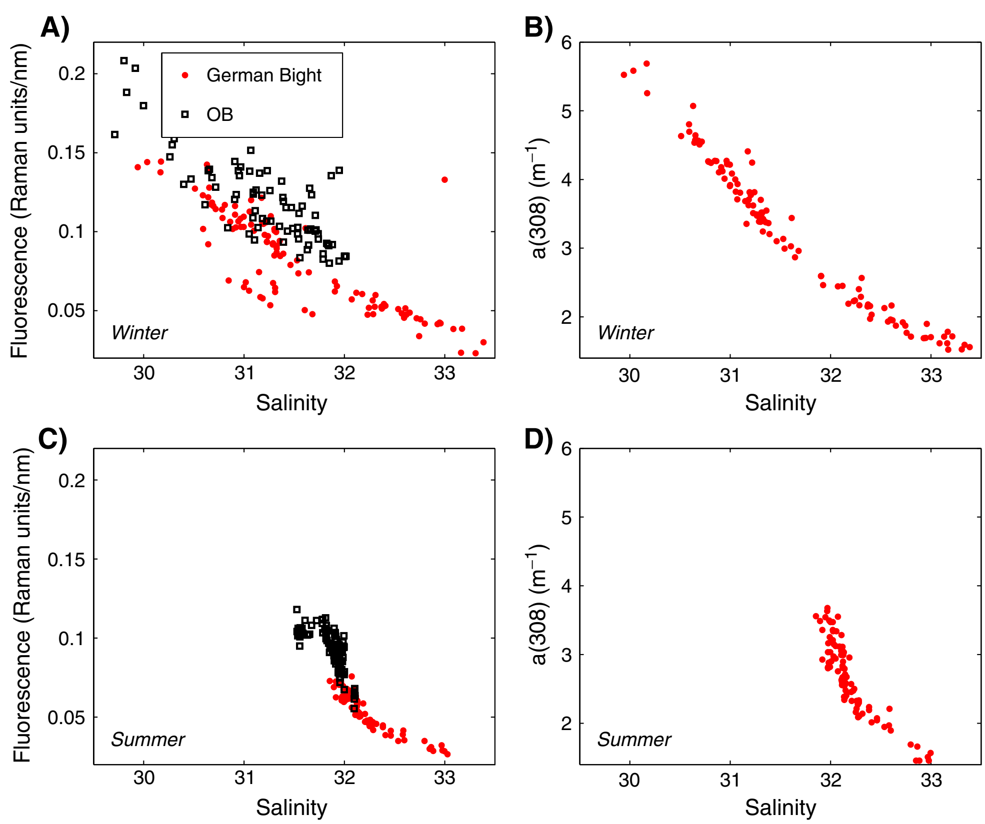

Fig. 8 CDOM fluorescence (λ_{ex}=308 nm, λ_{em}=420 nm) and absorption coefficients versus salinity of the German Bight (*red dots*) and the backbarrier area of the Island of Spiekeroog (*black squares*) in winter and summer

Strong tidal dynamics cause an intense water exchange between the German Bight and the adjoining backbarrier areas. Thus, coastal DOM-rich waters influenced by terrestrial run-off and pore water contribution are mixed with offshore waters of lower DOM content. The data suggest that both optical parameters do not behave completely conservative throughout the year as seen in the non-linear pattern which is most pronounced for the German Bight samples in summer. Whilst samples from the backbarrier area tend to reveal a linear mixing pattern, the German Bight waters display a certain break at a salinity of 31.8 in winter and 32.3 in summer. In contrast, correlations of fluorescence versus salinity in the North Sea and Dutch Wadden Sea were observed by Kalle (1949), Reuter et al. (1986, 1993) and Zimmermann and Rommets (1974). Additionally, mixing processes have been studied in many regions of the world, concluding that CDOM behaves conservatively (i.e. Callahan et al. 2004; Chen and Gardner 2004; Del Castillo et al. 1999; Hong et al. 2005; Rochelle-Newall and Fisher 2002; Vodacek et al. 1997). However, non-conservative mixing patterns were observed by several investigations as well. For instance, Chen et al. (2007) assessed both conservative and non-conservative mixing within a time span of a half year in Tampa Bay. The authors explained the observed non-linearity with a stronger influence of photo-bleaching which leads to a depletion of CDOM. Nieke et al. (1997) observed a linear behaviour of fluorescence and absorption coefficients over a wide salinity range (0–32) in the St. Lawrence estuary, but found a slope discontinuity at a salinity of about 29. In the German Bight photochemical degradation, evaporation and biological activity might lead to non-linear mixing as well, whilst pronounced tidal dynamics may obscure such effects in the backbarrier area.

When analysing the transects shown in Figs. 4 and 6, three water types can be identified in the study area. First, the low-salinity water near the coast showing high values of fluorescence, absorption coefficients and DOC. This water type is highly influenced by the pore water as well as by the terrestrial run-off. The plume is distributed up to 2 km afar from the harbour at low tide (see Fig. 4) and also observed at position OB18 (see Fig. 2), which is about 3 km north of the harbour of Neuharlingersiel. This kind of water type shows a conservative mixing behaviour over the complete salinity range. A second water type is the sea water of the German Bight which is characterised by high salinity of, on average, 33 and a low DOM content (fluorescence average 0.03 Raman units/nm; absorption coefficients average 1.5 m^{-1}). This kind of water type can be observed more than 20 km north off the islands. Between both types, a mixing zone develops due to tidal dynamics. This transitional water type is identified by medium values of fluorescence, absorption coefficient and salinity with some seasonal variability and a non-conservative behaviour during mixing.

4 Conclusions

The spatial distribution of DOM in the German Bight and the adjacent Wadden Sea shows a strong gradient from the open German Bight towards the coast. The temporal distribution evidences a dependence on tidal dynamics. The amount of DOM in the Wadden Sea increases during low water, whereas it decreases during high tide.

On the basis of our data, the complexity of DOM cycling in coastal regions is demonstrated. A couple of different sources and sinks influence CDOM and DOC budgets, each with different influencing factors depending on season. This might be the reason for DOM budgets being rare in the literature. The main sources of the East-Frisian Wadden Sea are terrestrial run-off via flood-gates as well as pore water, whereas the German Bight serves as a source during high tide and as a sink during ebb tide. For the investigation area, the importance of the pore water release should be studied in more detail in the future. Especially the discharge rates at tidal flat margins have to be better characterised. This enables to establish a mass balance. Furthermore, photochemical degradation, (micro)biological activity, aggregation and sedimentation of suspended matter, as well as evaporation impact the balance of DOM. The establishment of a mass balance requires a more detailed knowledge of the contributions of the specific sources and sinks.

Both parameters CDOM and DOC are decoupled throughout the year, especially during algae blooms and periods of enhanced microbial activity. Thus, the suitability of CDOM fluorescence and DOC as tracers for identifying different water types is limited. The behaviour of these parameters in the investigation area indicates both linear and non-linear mixing depending on the season.

Acknowledgements The authors would like to thank the crews of R/V Senckenberg and R/V Heincke for their assistance and facilitation during the cruises. We wish to thank I. Ötken and A. Braun for their helpful assistance with the sample collection and analysis. We are also grateful to L. Aden (Niedersächsischer Landesbetrieb für Wasserwirtschaft, Küsten- und Naturschutz, NLWKN) and J. Meinen-Hieronimus for providing the terrestrial run-off volumes via the flood-gates of Neuharlingersiel. The investigations are part of the research programme BioGeoChemistry of Tidal Flats funded by the Deutsche Forschungsgemeinschaft (DFG) through grants FOR 432/1-1, RE 624/5 and BR 775/14-1/2.

References

Beck M, Dellwig O, Kolditz K, Freund H, Liebezeit G, Schnetger B, Brumsack H-J (2007) In situ pore water sampling in deep intertidal flat sediments. Limnol Oceanogr Methods 5:136–144

Beck M, Dellwig O, Liebezeit G, Schnetger B, Brumsack H-J (2008a) Spatial and seasonal variations of sulphate, dissolved organic carbon, and nutrients in deep pore waters of intertidal flat sediments. Estuar Coast Shelf Sci 79:307–316, doi:10.1016/j.ecss.2008.04.007

Beck M, Dellwig O, Holstein JM, Grunwald M, Liebezeit G, Schnetger B, Brumsack H-J (2008b) Sulphate, dissolved organic carbon, nutrients and terminal metabolic products in deep pore waters of an intertidal flat. Biogeochemistry 89:221–238, doi:10.1007/s10533-008-9215-6

Beck M, Dellwig O, Schnetger B, Brumsack H-J (2008c) Cycling of trace metals (Mn, Fe, Mo, U, V, Cr) in deep pore waters of intertidal flat sediments. Geochim Cosmochim Acta 72:2822–2840, doi:10.1016/j.gca.2008.04.013

Billerbeck M, Werner U, Bosselmann K, Walpersdorf E, Huettel M (2006a) Nutrient release from an exposed intertidal sand flat. Mar Ecol Prog Ser 316:35–51, doi:10.3354/meps316035

Billerbeck M, Werner U, Polerecky L, Walpersdorf E, de Beer D, Huettel M (2006b) Surficial and deep pore water circulation governs spatial and temporal scales of nutrient recycling in intertidal sand flat sediment. Mar Ecol Prog Ser 326:61–76, doi:10.3354/meps326061

Breves W, Reuter R, Delling N, Michaelis W (2003) Fluorophores in the Arabian Sea and their relation to upwelling processes. Ocean Dyn 53:73–85, doi:10.1007/s10236-003-0025-z

Bricaud A, Morel A, Prieur L (1981) Absorption by dissolved organic matter of the sea (yellow substance) in the UV and visible domains. Limnol Oceanogr 26:43–53

Callahan J, Dai M, Chen RF, Li X, Lu Z, Huang W (2004) Distribution of dissolved organic mater in the Pearl River Estuary. Mar Chem 89:211–224, doi:10.1016/j.marchem.2004.02.013

Chang TS, Bartholomä A, Flemming BW (2006) Seasonal dynamics of fine-grained sediments in a back-barrier tidal basin of the German Wadden Sea (Southern North Sea). J Coast Res 22 (2):328–338, doi:10.2112/03-0085.1

Chen RF, Gardner GB (2004) High-resolution measurements of chromophoric dissolved organic matter in the Mississippi and Atchafalaya River plume regions. Mar Chem 89:103–125, doi:10.1016/j.marchem.2004.02.026

Chen Z, Hu C, Conmy RN, Muller-Karger F, Swarzenski P (2007) Colored dissolved organic matter in Tampa Bay, Florida. Mar Chem 104:98–109, doi:10.1016/j.marchem.2006.12.007

Coble PG (1996) Characterization of marine and terrestrial DOM in seawater using excitation–emission matrix spectroscopy. Mar Chem 51:325–346, doi:10.1016/0304-4203(95)00062-3

Coble PG, Green S, Blough NV, Gagosian RB (1990) Characterization of dissolved organic matter in the Black Sea by fluorescence spectroscopy. Nature 348:432–435, doi:10.1038/348432a0

Conmy RN, Coble PG, Chen R, Gardner GB (2004) Optical properties of colored dissolved organic matter in the Northern Gulf of Mexico. Mar Chem 89:127–144, doi:10.1016/j.marchem.2004.02.010

de Souza Sierra MM, Donard OFX, Lamotte M (1997) Spectral identification and behaviour of dissolved organic fluorescent material during estuarine mixing processes. Mar Chem 58:51–58, doi:10.1016/S0304-4203(97)00025-X

Dellwig O, Bosselmann K, Kölsch S, Hentscher M, Hinrichs J, Böttcher ME, Reuter R, Brumsack H-J (2007a) Sources and fate of manganese in a tidal basin of the German Wadden Sea. J Sea Res 57(1):1–18, doi:10.1016/j.seares.2006.07.006

Dellwig O, Beck M, Lemke A, Lunau M, Kolditz K, Schnetger B, Brumsack H-J (2007b) Non-conservative behaviour of molybdenum in coastal waters (Wadden Sea of NW Germany): coupling of biological, sedimentological, and geochemical processes. Geochim Cosmochim Acta 71:2745–2761, doi:10.1016/j.gca.2007.03.014

Del Castillo CE, Coble PG, Morell JM, Lopez JM, Corredor JE (1999) Analysis of the optical properties of the Orinoco River plume by absorption and fluorescence spectroscopy. Mar Chem 66:35–51, doi:10.1016/S0304-4203(99)00023-7

Del Vecchio R, Blough NV (2004) Spatial and seasonal distribution of chromophoric dissolved organic matter and dissolved organic carbon in the Middle Atlantic Bight. Mar Chem 89:169–187, doi:10.1016/j.marchem.2004.02.027

Determann S (1995) Analyse biologischer und biochemischer Prozesse im Meer mit Fluoreszenzspektroskopie. Carl von Ossietzky Universität Oldenburg, Diss

Determann S, Reuter R, Wagner P, Willkomm R (1994) Fluorescent matter in the eastern Atlantic Ocean. Part 1: method of measurement and near-surface distribution. Deep Sea Res Part I Oceanogr Res Pap 41(4):659–675, doi:10.1016/0967-0637(94)90048-5

Duursma EK (1974) The fluorescence of dissolved organic matter in the sea. In: Jerlov NG, Steeman Mielsen E (eds) Optical aspects of oceanography. Academic, London, pp 237–256

Ertel JR, Hedges JI, Devol AH, Richey JE, Ribeiro MNG (1986) Dissolved humic substances in the Amazon river system. Limnol Oceanogr 31:739–754

Flemming BW, Ziegler K (1995) High resolution grain size distribution patterns and textural trends in the backbarrier environment of Spiekeroog Island (southern North Sea). Senckenb Marit 26:1–24

Gebhardt S (2005) Organisch-geochemische Untersuchungen der Oberflächengewässer aus dem Einzugsgebietder Sielacht Esens (Ostfriesland). Carl von Ossietzky Universität Oldenburg, Diss

Gueguen C, Guo L, Tanaka N (2005) Distributions and characteristics of colored dissolved organic matter in the Western Arctic Ocean. Cont Shelf Res 25:1195–1207, doi:10.1016/j.csr.2005.01.005

Green SA, Blough NV (1994) Optical absorption and fluorescence properties of chromophoric dissolved organic matter in natural waters. Limnol Oceanogr 39:1903–1916

Hedges JI (1992) Global biogeochemical cycles: progress and problems. Mar Chem 39:67–93, doi:10.1016/0304-4203(92)90096-S

Hedges JI, Eglinton G, Hatcher PG, Kirchman DL, Arnosti C, Derenne S, Evershed RP, Kögel-Knabner I, de Leeuw JW, Littke R, Michaelis W, Rullkötter J (2000) The molecularly-uncharacterized component of nonliving organic matter in natural environment. Org Geochem 31:945–958, doi:10.1016/S0146-6380(00)00096-6

Hong H, Wu J, Shang S, Hu C (2005) Absorption and fluorescence of chromophoric dissolved organic matter in the Pearl River Estuary, South China. Mar Chem 97:78–89, doi:10.1016/j.marchem.2005.01.008

Huettel M, Rusch A (2000) Transport and degradation of phytoplankton in permeable sediment. Limnol Oceanogr 45(3):534–549

Huettel M, Ziebis W, Forster S, Luther GW (1998) Advective transport affecting metal and nutrient distributions and interfacial fluxes in permeable sediments. Geochim Cosmochim Acta 62 (4):613–631, doi:10.1016/S0016-7037(97)00371-2

Kalle K (1938) Zum Problem der Meerwasserfarbe. Ann Hydrol Mar Mitt 66:1–13

Kalle K (1949) Fluoreszenz und Gelbstoff im Bottnischen und Finnischen Meerbusen. Ocean Dyn 2:117–124, doi:10.1007/BF02225972

Kirk JTO (1988) Solar heating of water bodies as influenced by their inherent optical properties. J Geophys Res 93:10897–10908, doi:10.1029/JD093iD09p10897

Kirk JTO (1994) Light and photosynthesis in aquatic ecosystems. Cambridge University Press, Cambridge

Kölsch S, Gebhardt S, Terjung F, Liebezeit G, Reuter R, Rullkötter J, Brumsack H-J (2003) Freshwater discharge into the East Frisian Wadden Sea: geochemistry of humic matter-rich waters. Berichte—Forschungszentrum Terramare 12:71–74

Kouassi A, Zika R (1990) Light-induced alteration of the photophysical properties of dissolved organic matter in seawater. Neth J Sea Res 27(1):25–32, doi:10.1016/0077-7579(90)90031-B

Krause G, Budeus G, Gerdes G, Schaumann K, Hesse K (1986) Frontal systems in the German Bight and their physical and biological effects. In: Nihoul JCJ (ed) Marine interfaces ecohydrodynamics. Elsevier Oceanography Series 42, Elsevier, Amsterdam, pp 119–140

Lunau M, Lemke A, Dellwig O, Simon M (2006) Physical and biogeochemical controls of microaggregate dynamics in a tidally affected coastal ecosystem. Limnol Oceanogr 51:847–859

Malcolm RL (1990) The uniqueness of humic substances in each of soil, stream ans marine environments. Ann Chem Acta 232:19–30, doi:10.1016/S0003-2670(00)81222-2

Miller WL, Moran MA (1997) Interaction of photochemical and microbial processes in the degradation of refractory dissolved organic matter from a coastal marine environment. Limnol Oceanogr 42(6):1317–1324

Mopper K, Schultz CA (1993) Fluorescence as a possible tool for studying the nature and water column distribution of DOC components. Mar Chem 41:229–238, doi:10.1016/0304-4203(93)90124-7

Moran MA, Hodson RE (1994) Dissolved humic substances of vascular plant origin in a coastal marine environment. Limnol Oceanogr 39(4):762–771

Moran MA, Sheldon WM Jr, Zepp RG (2000) Carbon loss and optical property changes during long-term photochemical and biological degradation of estuarine dissolved organic matter. Limnol Oceanogr 45(6):1254–1264

Muller-Karger FE, McClain CR, Fisher TR, Esaias WE, Varela R (1989) Pigment distribution in the Caribbean Sea: observation from space. Prog Oceanogr 23:23.64

Nieke B, Reuter R, Heuermann R, Wang H, Babin M, Therriault JC (1997) Light absorption and fluorescence properties of chromophoric dissolved organic matter (CDOM), in St. Lawrence Estuary (Case2 waters). Cont Shelf Res 17(3):235–252, doi:10.1016/S0278-4343(96)00034-9

Niesel V, Günther CP (1999) Distribution of nutrients, algae and zooplankton in the Spiekeroog backbarrier system. In: Dittmann S (ed) The Wadden Sea ecosystem—stability properties and mechanisms. Springer, Berlin, pp 77–94

NLWKN (2000) Nährstoffeinträge in die Nordsee, Niedersächsischer Landesbetrieb für Wasserwirtschaft und Küstenschutz-Betriebsstelle Aurich

NLWKN (2004) Ermittlung von Abflüssen über Siel- und Pumpmengen in Ostfriesland, Niedersächsischer Landesbetrieb für Wasserwirtschaft und Küstenschutz-Betriebsstelle Aurich

Opsahl S, Benner R (1998) Photochemical reactivity of dissolved lignin in river and ocean waters. Limnol Oceanogr 43(6):1297–1304

Puncken O, Badewien T, Reuter R (2006) MOSES (measuring system for the observation of sea surfaces): Lagrangian drift experiments in the East Frisian Wadden Sea. In: Marcal A (ed) Global developments in environmental earth observation from space. Millpress, Rotterdam, The Netherlands, pp 697–706

Reuter R, Diebel-Langohr D, Doerffer R, Dörre F, Haardt H, Hengstermann T (1986) Optical properties of gelbstoff. In: The influence of yellow substances on remote sensing in seawater constituents from space, vol 2. GKSS Forschungszentrum Geesthacht, Germany, 58ff

Reuter R, Diebel D, Hengstermann T (1993) Oceanographic laser remote sensing: measurements of hydrographic fronts in the German Bight and in the Northern Adriatic Sea. Int J Remote Sens 14(5):823–848, doi:10.1080/01431169308904380

Rochelle-Newall EJ, Fisher TR (2002) Chromophoric dissolved organic matter and dissolved organic carbon in Chesapeake Bay. Mar Chem 77:23–41, doi:10.1016/S0304-4203(01)00073-1

Shaw TJ (2003) Methods and models for estimating advective pore water exchange in tidal flats. Berichte—Forschungszentrum Terramare 12:103–104

Skoog A, Hall POJ, Hulth S, Paxéus N, Van Der Loeff MR, Westerlund S (1996) Early diagenetic production and sediment–water exchange of fluorescent dissolved organic matter in the coastal environment. Geochim Cosmochim Acta 60(19):3619–3629, doi:10.1016/0016-7037(96)83275-3

Spitzy A, Ittekkot V (1986) Gelbstoff: an uncharacterized fraction of dissolved organic carbon. In: The influence of yellow substances on remote sensing of seawater constituents from space, volume II, Appendix 1, 31 pp. ESA Contract No. RFQ 3-5060/84/NL/MD, GKSS Forschungszentrum Geesthacht, Germany, December 1986

Stanev EV, Wolff J-O, Burchard H, Bolding K, Flöser G (2003) On the Circulation in the East Frisian Wadden Sea: numerical modeling and data analysis. Ocean Dyn 53(1):27–51, doi:10.1007/s10236-002-0022-7

Sündermann J, Hesse K-J, Beddig S (1999) Coastal mass and energy fluxes in the southeastern North Sea. Ocean Dyn 51:113–132

Traganza ED (1969) Fluorescence excitation and emission spectra of dissolved organic matter in sea water. Bull Mar Sci 19:897–904

Velapoldi RA, Mielenz KD (1980) A fluorescence standard reference material: quinine sulphate dihydrate. NBS Special Publication SP 260-64. National Bureau of Standards, Washington DC, 139 pp. Available at http://ts.nist.gov/MeasurementServices/ReferenceMaterials/upload/SP260-64.PDF

Vodacek A, Blough NV, DeGrandpre MD, Peltzer ET, Nelson RK (1997) Seasonal variation of CDOM and DOC in the Middle Atlantic Bight: terrestrial inputs and photooxidation. Limnol Oceanogr 42(4):674–686

Volkenborn N, Polerecky L, Hedtkamp SIC, van Beusekom JEE, de Beer D (2007) Bioturbation and bioirrigation extend the open exchange regions in permeable sediments. Limnol Oceanogr 52:1898–1909

Wolff J-O, Flemming BW (2003) Tidal asymmetries, water exchanges and sediment transports in the East Frisian Wadden Sea. Berichte—Forschungszentrum Terramare 12:132–137

Zimmermann JTF, Rommets JW (1974) Natural fluorescence as a tracer in the Dutch Wadden Sea and adjacent North Sea. Neth J Sea Res 8:117–125, doi:10.1016/0077-7579(74)90012-X